applied sciences

MDPI

Article

Fusion of Unobtrusive Sensing Solutions for Home-Based Activity Recognition and Classification using Data Mining Models and Methods

Idongesit Ekerete[1], Matias Garcia-Constantino[1], Alexandros Konios [2], Mustafa A. Mustafa[3,4], Yohanca Diaz[5], Chris Nugent[1] and Jim McLaughlin[6]*

[1] School of Computing, Jordanstown Campus, Ulster University, United Kingdom.
[2] School of Digital, Technologies and Arts, Staffordshire University, United Kingdom.
[3] Department of Computer Science, The University of Manchester, United Kingdom.
[4] imec-COSIC, KU Leuven, Leuven, Belgium.
[5] Dundalk Institute of Technology, NetwellCASALA, Dundalk Institute of Technology, Rep. of Ireland.
[6] School of Engineering (NIBEC), Jordanstown Campus, Ulster University, United Kingdom.
* Correspondence: ekerete-i@ulster.ac.uk; Tel.:+447438315653

Abstract: This paper proposes the fusion of Unobtrusive Sensing Solutions (USSs) for human Activity Recognition and Classification (ARC) in home environments. It also considers the use of data mining models and methods for cluster-based analysis of datasets obtained from the USSs. The ability to recognise and classify activities performed in home environments can help monitor health parameters in vulnerable individuals. This study addresses five principal concerns in ARC: (i) users' privacy, (ii) wearability, (iii) data acquisition in a home environment, (iv) actual recognition of activities, and (v) classification of activities from single to multiple users. Timestamps information from contact sensors mounted at strategic locations in a kitchen environment helped obtain the time, location and activity of 10 participants during the experiments. 11,980 thermal blobs gleaned from privacy-friendly USSs such as ceiling and lateral thermal sensors were fused using data mining models and methods. Experimental results demonstrated cluster-based activity recognition, classification and fusion of the datasets with an average regression coefficient of 0.95 for tested features and clusters. In addition, a pooled Mean accuracy of 96.5% was obtained using classification-by-clustering and statistical methods for models such as Neural Network, Support Vector Machine, K-Nearest Neighbour and Stochastic Gradient Descent on Evaluation Test.

Keywords: K-Means Analysis; Home Environment; Sensor Fusion; Activity Recognition; Unobtrusive Sensing; Data Mining; Principal Component Analysis; Infrared Thermopile Array.

Citation: Lastname, F.; Lastname, F.; Lastname, F. Title. *Appl. Sci.* **2021**, *11*, x. https://doi.org/10.3390/xxxxx

Academic Editor: Firstname Lastname

Received: date
Accepted: date
Published: date

1. Introduction

Recognising individual activities of people susceptible to hazardous behaviours such as falls, wandering, and agitation has been an active research topic, which has witnessed the use of pervasive and non-pervasive Sensing Solutions (SSs) [1]. This paper is an extended version of the paper "Data Mining and Fusion of Unobtrusive Sensing Solutions for Indoor Activity Recognition", published in 2020 42nd Annual International Conference of the IEEE Engineering in Medicine & Biology Society (EMBC) [2]. Interestingly, many cases of hazardous behaviours in ageing adults can be prevented [3] [4]. While there are several SSs that can detect these behaviours when they occur, it would be of great benefit if they can be predicted prior to their occurrence. This may be achieved by using Data Mining (DM) and Machine Learning (ML) models, which can help discover patterns and potential deviations from established patterns in the data gleaned from a sensorised environment.

Pattern Deviation Assessment (PDA) in activity recognition is a vital tool in detecting abnormal activities [5]. Its outcome helps to determine if an ageing individual can be considered to be independent or not whilst performing certain activities [5]. This is an important part of the home-based assessment process to gauge if a person can remain living in their own home. PDA can also help determine the extent of recovery from injury, potential hazardous behaviour and an individual's effectiveness. Pattern deviation can take forms such as detecting incomplete activities and sudden changes in activity, disposition and posture. PDA outcomes are often positioned in clusters to help access a set of activities or patterns on demand. The present work benefits from cluster-based analysis of patterns discovered from features extracted from thermal images using DM models and methods.

Research in ARC has often considered the use of wearables such as accelerometers and video-based solutions such as Kinect [6]–[12]. Whilst accelerometers can provide information on orientation and angular acceleration of the worn part, wearability and data disruptions are some of the disadvantages. Likewise, Kinect has problems ranging from interference with external infrared sources to privacy and reflections in home environments [13]–[16]. This work tackles these problems through the usage of Unobtrusive Sensing Solutions (USSs) such as Infrared Thermopile Array (ITA) thermal SSs, which are non-wearable and not prone to reflections in home environments.

The novel contributions of this work are four-fold. First, it presents an unobtrusive data collection through the use of non-wearable (i.e., privacy-friendly) USSs. Secondly, it presents a comprehensive analysis of the data gleaned from two ITA sensors through the use of DM models and methods. Thirdly, it proposes the fusion of data from the ceiling and lateral thermal sensors to address instances of occlusion. Fourthly, it compares the averages of models from the lateral, ceiling and fused datasets using statistical methods such as T-Test and ANOVA.

The remainder of this paper is organised as follows: Section 2 discusses related work; Section 3 presents the materials and methods; Section 4 presents the experimental results; Section 5 presents discussions around the study findings and conclusions.

2. Related Work

Many SSs have been deployed over the years for the purposes of activity recognition [17]–[19]. These have included the use of wearable or non-wearable solutions or the fusion of both. Whilst they help data acquisition in the environment where they are deployed, their use in home settings can be negatively influenced by signals from other legacy systems and obstructive materials. Work in [20] proposed the use of a Hidden Markov Model to recognise human activities based on data gleaned from a waist-worn accelerometer. The model also classified collected signals according to a corresponding class. In the study, continuous monitoring was performed by a Gaussian Mixture Model.

A further study by Ni *et al.* [21] used a Multivariate Online Change Detection algorithm for activity recognition.

Accelerometers for activity recognition have been featured in many studies [20], [22]. In [23], the use of tri-axial accelerometers was proposed for monitoring rest, movement, transition and emergency states in ageing adults. Although the successful detections of the activities were noted in the study, the ability to distinguish between activities and classify them accordingly was considered for further improvements. In [24], a tri-axial accelerometer was used to monitor daily physical activity. In addition to the challenges of the approach presented in [23], wearability was an issue reported in the latter study. Another multi-wearable sensor study was carried out by Gao *et al.* [22]. Whilst a garment-based accelerometer might exhibit improved performance in a laboratory environment as illustrated by [22], real-life usage may suffer the risks of explosion or damage to the sensors during washing activity. Also, long term usage can cause a feeling of discomfort for the user.

Activity Recognition and Classification (ARC) through the use of mobile devices has also been researched [2]. Work by Figo *et al.* [8] explored the use of a smartphone's accelerometer to recognise and classify activities such as running and walking during a certain period of the day. The study obtained information from the GPS sensor to suggest to the user routines similar to those performed in previous days. The work presented by [25] suggested that mobile devices should be optimised to enhance the continuous monitoring and processing of data acquired from their sensors. Whilst these suggestions seem innovative and worthy of exploration, battery life and the users' ability to remember to carry mobile devices around are major setbacks. Furthermore, in Konios *et al.* [26], a probabilistic examination of temporal and sequential aspects of activities using an approach based on the Cumulative Distribution Function is employed to determine abnormalities in activities. This approach involved deriving probabilities of normal behaviours with respect to the duration and the stages of an activity. Whilst this study introduced an effective way to detect (ab)normal activities, a profile analysis of users aimed at ensuring more precision in detecting the presence of health-related abnormalities is still being researched.

Data fusion from homogeneous and heterogenous sensors has also been deployed in ARC. Garcia-Constantino *et al.* [18] investigated the fusion of data from wearable (accelerometer) and ambient (thermal) sensors by extracting relevant features from both. Initial results from this approach indicated an improvement in abnormal behaviour detection.

DM and ML models have positively influenced human activity recognition, clustering and classification in home settings. Whilst many activity monitoring models can exhibit excellent performance in a controlled environment such as laboratories [21], others can only be moderated by trained personnel [27]. This often results in successful laboratory work which cannot be deployed in a real-life setting.

Presently, ARC in a home environment has featured sophisticated SSs. These solutions are often used to acquire data in different areas, including the prediction of prevalence and management of individuals with diseases such as dementia, osteoporosis, and increased fragility [28], [29]. They also help to detect hazardous incidents [19]. Nevertheless, data acquisition in a home setting can be negatively influenced by gadgets that can interfere with signal propagation from different SSs. Whilst the many advantages of using a video camera for home monitoring solutions cannot be understated, lack of privacy protection and changes in lighting conditions are the main concerns for its use. This study was performed to address five principal concerns in ARC: (i) users' privacy, (ii) wearability, (iii) data acquisition in a home environment, (iv) actual recognition of activities, and (v) classification of activities from single to multiple users. Hence, this study presents the fusion of data from unobtrusive (i.e., privacy-friendly) SSs for home-based ARC using DM models and methods.

3. Materials and Methods

Research in human activity recognition is an important monitoring process in smart homes [27] that has witnessed the use of wearable and non-wearable SSs. In this study, attention was given to privacy-friendly USSs. Also, the study was carried out in a smart laboratory kitchen that mimics a typical home kitchen [30]. More than 11,000 thermal blobs were recorded from 10 participants with two Infrared Thermopile Array (ITA) sensors. Participants were asked to prepare either a cup of tea or coffee.

The present work uses two ITA-32 sensors to monitor and recognise activities in a laboratory kitchen, which is similar to a home kitchen. The two thermal sensors are used simultaneously to address instances of missing thermal blobs due to occlusion. Automated processing techniques are used to synchronise and extract features and to fuse data from both sensors. Contact sensors are used as the baseline to compare their timestamps with those of thermal sensors. The study was carried out in a laboratory kitchen (Figure 1), which measures 3.9m by 3.4m. Ten healthy participants took part in the study, and each of them participated in a total of seven experiments. To have a more realistic scenario, participants were allowed to take as long as they wished to complete the activities in each experiment. There were no time constraints or control on the duration of the activities undertaken.

Pictorial View of Laboratory Kitchen Used for the Study

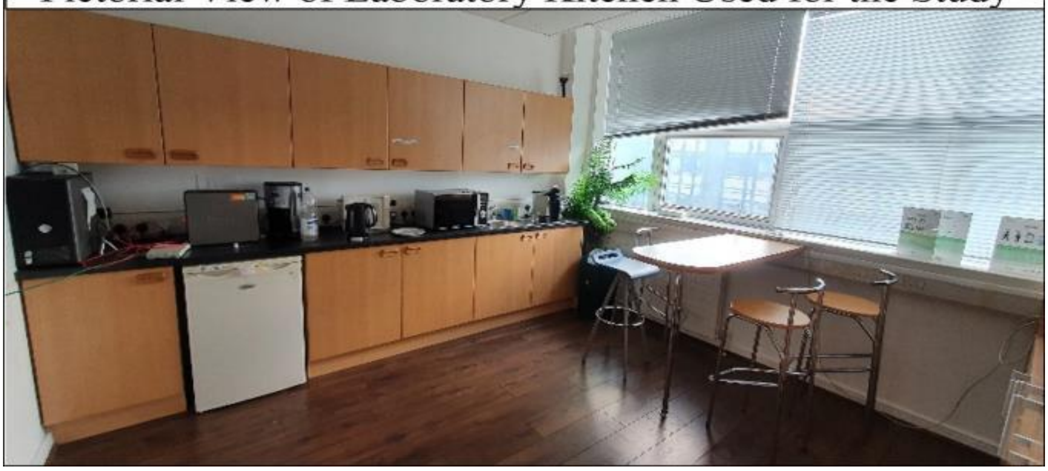

Figure 1. Pictorial View of the smart laboratory kitchen used for the study. A detailed description of the kitchen layout is presented in Figure 2.

The laboratory kitchen is comprised of cupboards (labelled 1– 4 in Figure 2) where tea, coffee, cups and sugar were stored. Underneath the cupboards is a worktop with a microwave, a kettle and a sink, thus mimicking a real-life kitchen. A refrigerator is located on the floor beneath the worktop, as indicated in Figure 2. The main kitchen area is where participants walked around to prepare a hot beverage (either tea or coffee) which was then taken to the table area for consumption.

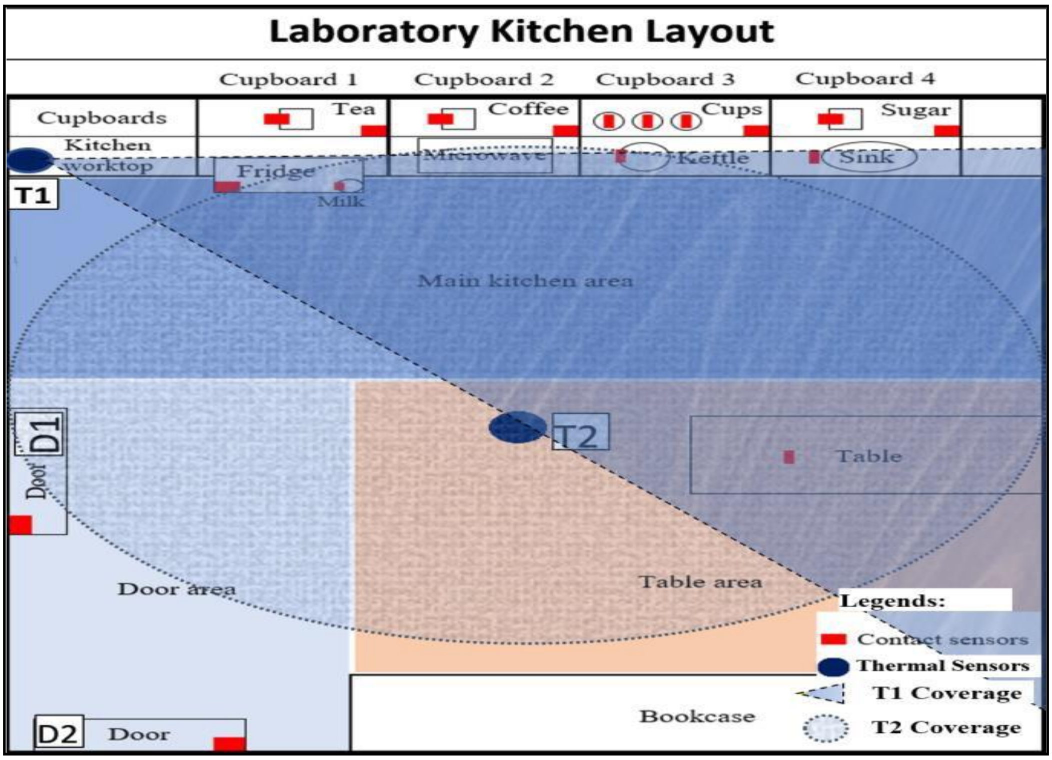

Figure 2. Laboratory Kitchen Layout. The areas marked in red indicate the location of the contact sensors. Thermal sensors are indicated by the navy-blue oval shape as T1 and T2 for lateral and ceiling thermal sensors, respectively. The coverage of T1 is indicated by the triangular area while that of T2 is indicated by the oval area.

In Figure 2, the lateral and the ceiling SSs are represented as T1 and T2, respectively. Whilst T1's indicative coverage included a half of the kitchen area as represented by the triangular shades in Figure 2, T2's coverage included a larger portion of the kitchen area as indicated by the oval shades. During data acquisition, each participant (at a time) walked in through door D1 to the main kitchen area where the cups were located. While some participants preferred to boil water in the kettle before going for the cups, others did the opposite. Data acquisition began a few seconds prior to opening door D1, notwithstanding the activity preferences of the participants.

Data from T1 and T2 were stored in a bespoke time-series database referred to as *SensorCentral* [31], [32]. A total of 11,980 frame data (1,198 from each participant) were collected from the seven experiments. The contact sensors, which were also associated with the database, were able to record the times when each activity began and ended. Moreover, contact sensors were used as the baseline to compare the timestamps of both types of sensors. They also help to indicate which of the participants had tea or coffee. DM tools and algorithms were used to extract features and to fuse data from both sensors. The DM algorithms used included the Hierarchical Clustering Algorithm (HCA) and the K-Means Algorithm (KMA). Metrics such as Classification Accuracy (CA), Specificity, weighted average (F1), Recall and Area Under the Curve (AUC) were used the ascertain the performance of DM models such as K-Near Neighbors (KNN), Logistic Regression (LR) and Neural Network (NN). Others included Random Forest (RF), Stochastic Gradient Descent (SGD), and Support Vector Machine (SVM).

4. Results

Experimental results indicated that activities such as using a bottle of milk could be identified and distinguished from using a kettle of hot water (Figure 3) using thermal blobs from T1. While a bottle of milk was seen as monochromatic shades of black due to its low temperature, a kettle of hot water had shades of white representation due to its high temperature, as presented in Figure 3. Moreover, it is important to note that notwithstanding the closeness of the participants to the thermal sensor (Figure 3), their identities were still protected. The RGB equivalents of the activities such as opening the fridge (Figure 4 (a)), heating a hot kettle (Figure 4(b)) and having a tea or coffee at the kitchen table (Figure 4(c)) are also presented for comparative purposes.

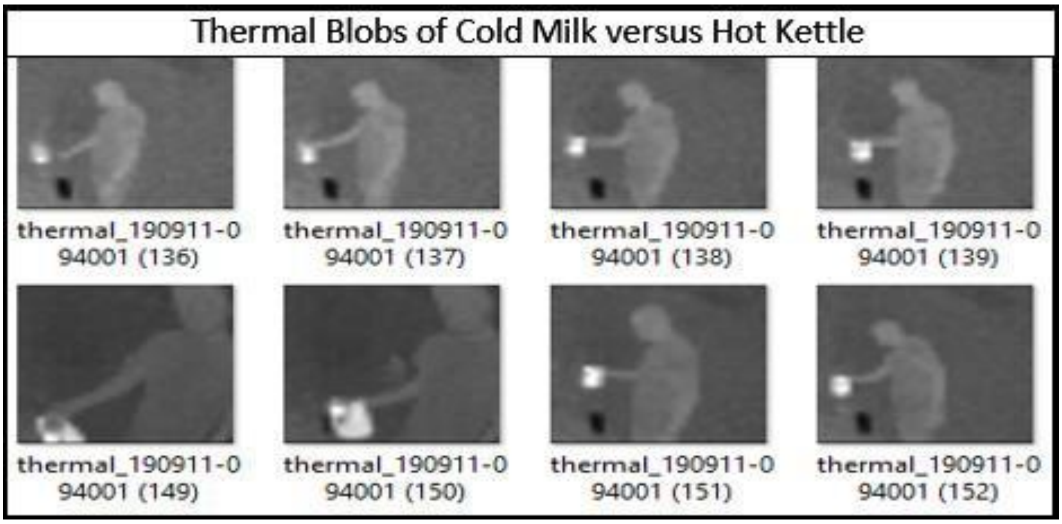

Figure 3. Thermal blobs of a bottle of cold milk (shades of black) distinguishable from a hot kettle (shades of white).

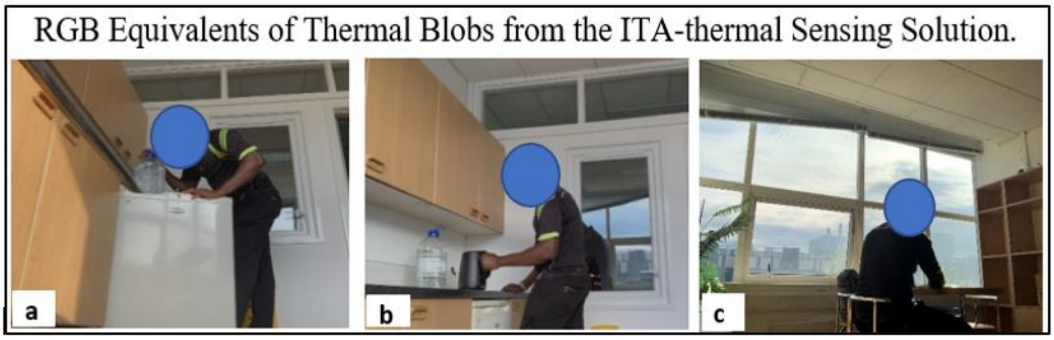

Figure 4. The RGB equivalents of activities: (a) opening the fridge, (b) heating a hot kettle, and (c) having tea or coffee at the kitchen table.

After preparing a cup of tea, it was easier to know from the thermal blobs whether the user successfully reached the table. In addition, it was necessary to know where the participant placed the hot kettle (after using it), which is a potential hazardous object. As presented in Figure 5, these activities were clearly viewed on the thermal image. Whilst the hot kettle was represented as a large blob adjacent to the participant, the tea/coffee cup was viewed as a small bright spot in what could be viewed as the hand of the user (Figure 5).

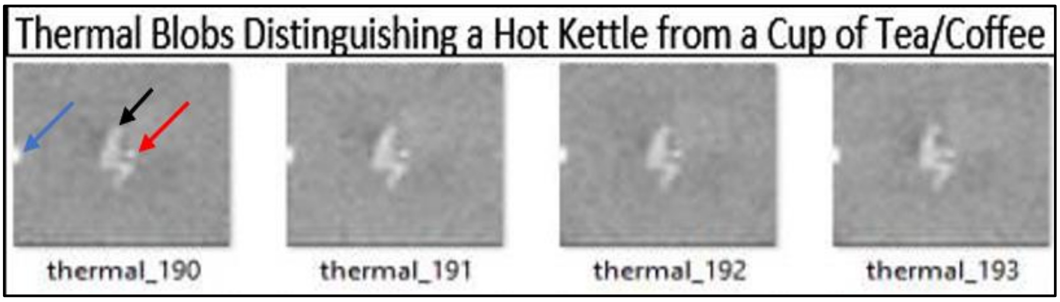

Figure 5. Distinguishable thermal blobs. On thermal_190, the blue arrow points to the hot kettle; the black arrow points to the participant and the red arrow to the tea/coffee cup after the initial act of tea/coffee making.

In some instances, the heat spot of a cup or kettle may be occluded by a participant when it is viewed from the lateral thermal sensor (see, Figure 6). When this happens, abnormal behaviours or activities may go unnoticed. To address these concerns, the ceiling sensor (T2) can be used to collect an aerial view as presented in Figure 7. Hence, the essence and usefulness of dual sensing in this study.

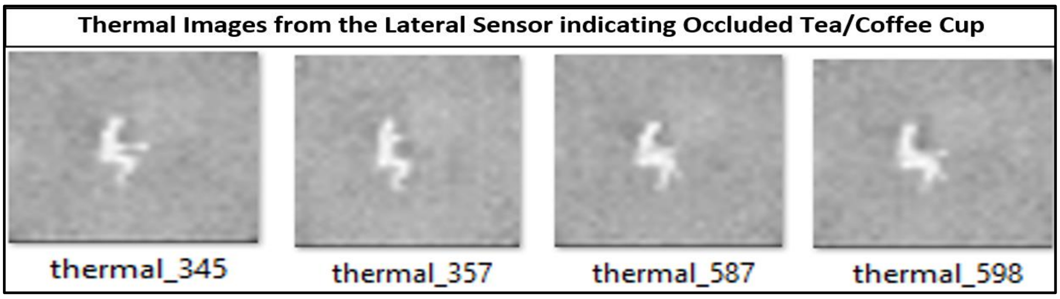

Figure 6. Thermal images from the lateral sensor indicating instances of occluded tea/coffee cups that are visible on the ceiling sensor. Refer to the thermal blobs with the same name as thermal_345, thermal_357, thermal_587, and thermal_598 in Figure 7.

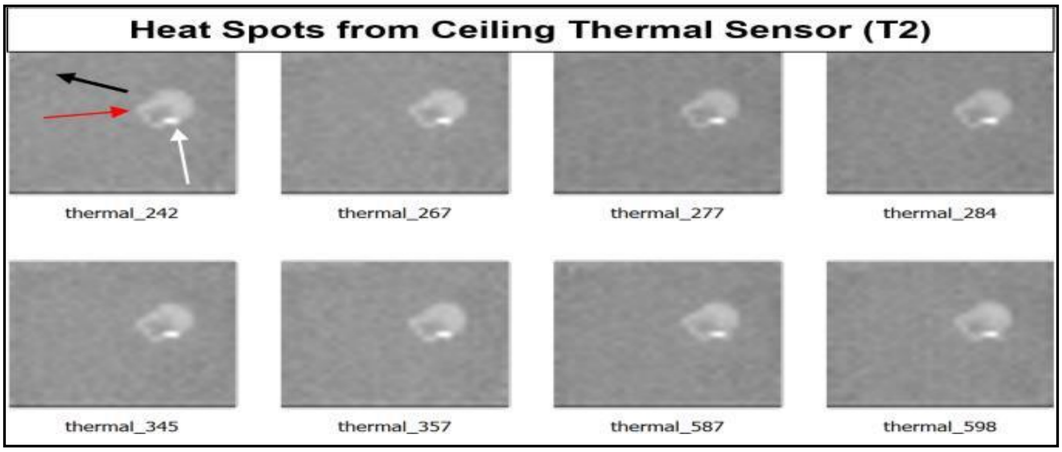

Figure 7. Heat Spots from tea/coffee cups occluded from the lateral thermal sensor (T1) but indicated by the ceiling thermal sensor (T2). The black arrow on thermal_242 points to the location of T1; the white arrow points to the heat spot and the red arrow points to the hand of the participant (occluding the heat spot).

4.1. Sensor Data Fusion

Sensor fusion using DM tools helps extract, cluster features and merge data from both SSs. A block diagram of the sensor data fusion architecture employed in this study is presented in Figure 8 [33].

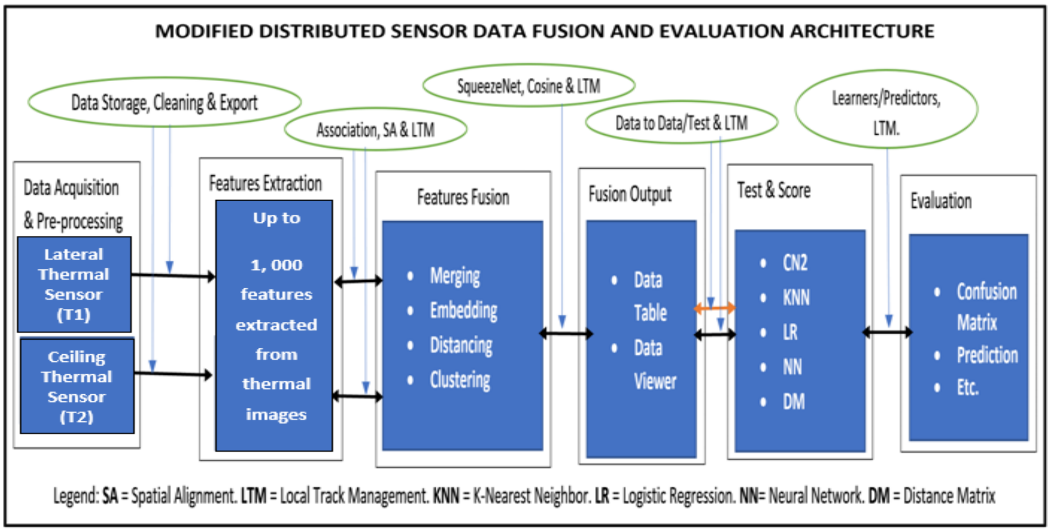

Figure 8. Modified Distributed Sensor Data Fusion Architecture for lateral (T1) and ceiling (T2) thermal sensors.

In Figure 8, data acquisition and pre-processing are performed by individual thermal sensors (T1 and T2). Up to 1,000 features are extracted from the thermal (grayscale and binary) images. Thermal blobs gleaned from the ITA sensors are stored in a predetermined folder with timestamps to enable a time-based fusion of the data. During sensor fusion, data from T1 and T2 were imported into the data merging system. The system then created an imaginary table for the two sets of data before carrying out a matching row appending. Whilst file-import enables the reading of tabular data and their instances from an Excel spreadsheet or a text document, the image-import toolkit helps upload images from folders. Information such as image width, size, height, path and name are automatically appended to each image uploaded in a tabular format.

Preliminary feature extraction was programmed to begin automatically. To ensure that the features are correctly matched, a matching row appending was used. Moreover, definitive feature extraction takes place at a data embedding capsule where more than 1,000 features, represented as vectors (n_0 to n_{999}), are extracted from each ITA image. The extraction was performed by using the SqueezeNet architecture, a deep neural network model for image recognition [33]. Unlike many sensor fusion or classification architectures that manually allocate clusters to images, the Louvain clustering algorithm [33] was used alongside distance metrics to automatically detect clusters. One of the advantages of using Louvain clustering is that of determining the number of clusters detected. The Louvain clustering algorithm further detect and integrate communities into the module. It also converts grouped features into a KNN graph and optimises their structures to obtain nodes that are interconnected.

Distance metrics, such as the cosine rule, was utilised in the Distances Application (DA). Also, feature normalisation, which performed column-wise normalisation for both categorical and numerical data, was applied [33]. The output of DA was connected to the hierarchical clustering module for the classification of the distanced features. Moreover, a dendrogram corresponding to a cluster of similar features from the DA was computed using the HCA. The clusters were primarily affected by resolution and Principal Component Analysis (PCA) parameters. In essence, increasing any of these parameters resulted in a corresponding decrease in the number of clusters that the algorithm detected. Data fusion outputs were viewed using a scatterplot, a data table and a data viewer widget.

One of the advantages of the sensor data fusion architecture proposed in this study includes viewing clusters comprising of all similar activities as presented in Figure 9, even if the activity was performed at different times by different participants. In Figure 9, for example, it could be easily deduced that a participant code-named C_ID was at the kitchen table with a hot cup of tea/coffee on the 8th of May 2019 at a different date and time as another participant code-named C_OR. With this information, activities can be easily monitored in clusters, notwithstanding the times and dates they were performed.

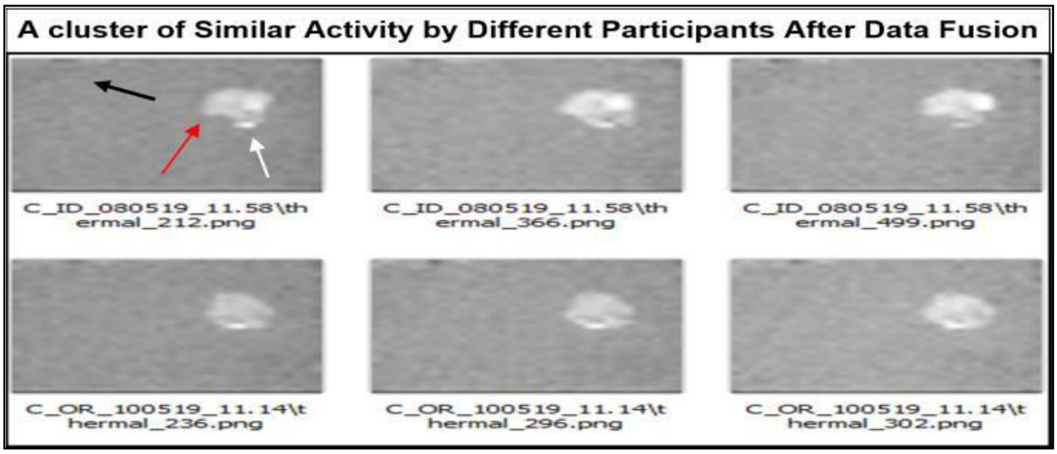

Figure 9. A cluster of data fusion output showing thermal blobs from two participants in a cluster with timestamps. The black arrow on 'C_ID_080519_11.58\thermal_212.png' points to the location of the lateral sensor; the red arrow points to the participant and the white arrow points to the heat spot from tea/coffee cup.

It is important to note that up to 1,000 features (labelled n_0 to n_{999}) were extracted from each thermal image during the feature extraction process. Using these features, a PCA and scoring of the clusters performed between features n525 and n830 at 99% variance coverage indicated a regression coefficient (r) of 0.98 and 1.00 for clusters 2 and 12, respectively as presented in Figure 10.

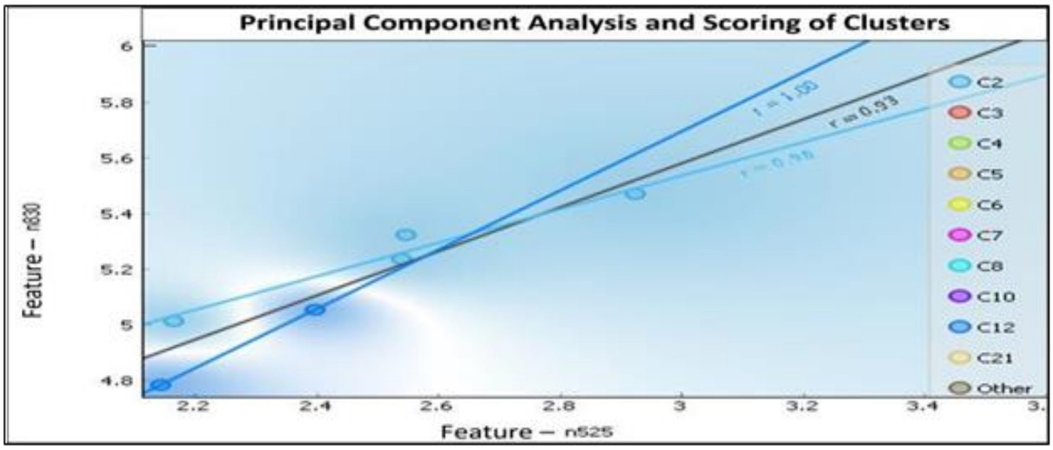

Figure 10. Features-based Principal Component Analysis and Scoring of Clusters. Features n525 and n830 are indicated on the X and Y axes, respectively. The clusters are color-coded, and the color of each regression line on the graph matches the color on the cluster legend on the right.

Similarly, a PCA and scoring analysis performed between features n246 and n170 for clusters 1, 6 and 9 yielded (r) of 0.83, 0.99 and 1.00, respectively, as presented in Figure 11. These resulted in an average (r) of 0.95 for all the tested features and clusters which were randomly selected from the HCA interface.

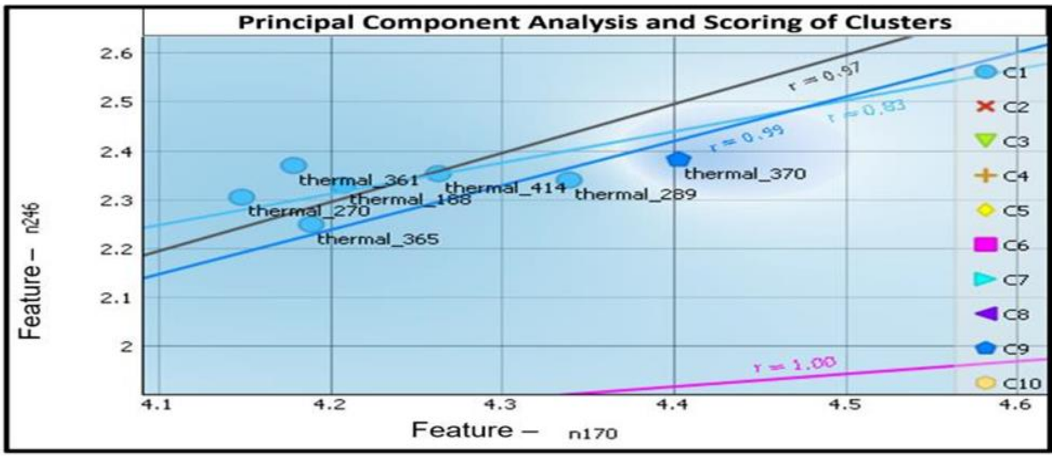

Figure 11. Features-based Principal Component Analysis and Scoring of Clusters. Features n170 and n246 are indicated on the X and Y axes, respectively. Also, the clusters are colour-coded, and the colour of each regression line on the graph matches the colour on the cluster legend on the right.

To further ascertain the certainty of the predicted clusters, an Evaluation Test was performed on all the clusters in the HCA using the KNN, LR, NN and RF models. While KNN yielded the lowest CA of 85.0%, LR and NN gave CAs of 96.1% and 100.0%, respectively, as presented in Table 1. In addition, the proportion of true positives of the positively classified instances (Precision) followed a similar trend as the CA. Furthermore, the NN yielded a value of 100.0% for the AUC, F1, CA, Precision, Recall and Specificity followed by RF with an average of 99.7%, as presented in Table 1.

Table 1. Evaluation results from data mining models for parameters such as AUC, CA, FI, Precision, Recall, LogLoss and Specificity.

Models	AUC (%)	CA (%)	F1 (%)	Precision (%)	Recall (%)	LogLoss (%)	Specificity (%)
KNN	99.1	85.0	85.0	85.4	85.0	0.3	98.3
LR	99.9	96.1	96.1	96.1	96.1	0.2	99.6
NN	100.0	100.0	100.0	100.0	100.0	0.0	100.0

RF	100.0	98.9	98.9	98.9	98.9	0.3	99.9
Average	**99.7**	**95.0**	**95.0**	**95.1**	**95.0**	**0.2**	**99.4**
Legend	KNN = K-Nearest Neighbours, LR = Logistic Regression, NN = Neural Network, RF = Random Forest, CA = Classification Accuracy, and AUC = Area Under the Curve.						

LogLoss, also referred to as cross-entropy loss, accounts for the performance of the classification model with respect to its variation from the actual label and was relatively low (less than 0.4%) for all the models (Table 1). NN had the most negligible value of 0.001%. While an average regression coefficient of 0.95 was obtained in the PCA and scoring test, an average accuracy of 96.5% was obtained for all the metrics (in Table 1) in the Evaluation Test.

Another demonstration of the accuracy of the architecture was in the analysis of the ceiling and lateral thermal sensors data using K-Means Clustering Method (KMCM). The KMCM is rated as a useful tool capable of providing quantitative and qualitative insight in multivariate analysis [34]. The data fusion and evaluation architecture based on the KMCM [35], is presented in Figure 12.

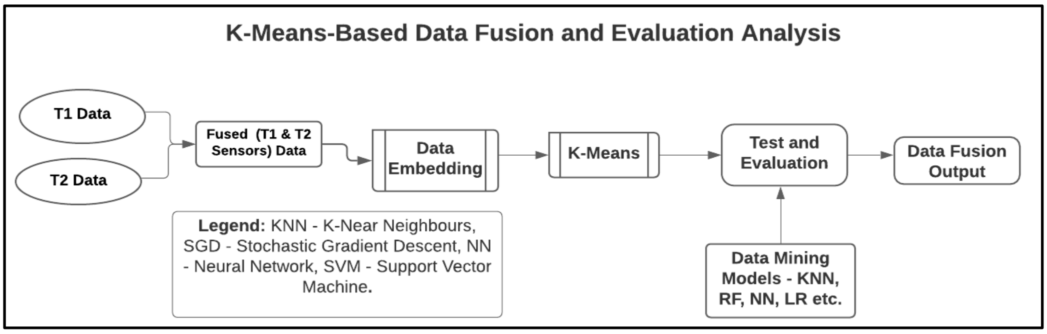

Figure 12. Simplified data fusion architecture based on K-Means Clustering Method (KMCM).

The KMCM-based architecture (Figure 12) fused thermal blobs data from thermal sensors T1 and T2. The fusion toolkit was linked directly to the image embedder. At the embedder, Inception V3, Google's ImageNet trained model [36] was used to embed the thermal blobs. KMA performed a maximum of 300 iterations of the data after columns normalisation in the K-Means toolkit. The output from the K-Means toolkit was used to train DM models such as KNN, NN, SGD, and SVM based on 66% training-set size. The evaluation result from the analysis based on a 10-fold cross-validation is presented in Table 2.

Table 2. K-Means evaluation results for fused datasets (F1) using data mining models such as KNN, SGD, NN and SVM.

Models	**AUC (%)**	**CA (%)**	**F1 (%)**	**Precision (%)**	**Recall (%)**	**LogLoss (%)**	**Specificity (%)**
KNN	98.8	91.8	91.9	92.0	91.8	0.1	99.6
SGD	97.6	95.5	95.5	95.5	95.5	0.0	99.8
NN	99.9	96.7	96.7	96.7	96.7	1.5	99.8
SVM	99.9	96.0	96.0	96.0	96.0	0.1	99.8
Average	**99.1**	**95.0**	**95.0**	**95.1**	**95.0**	**0.4**	**99.8**
Legend	KNN = K-Nearest Neighbours, NN = Neural Network, SGD = Stochastic Gradient Descent, SVM = Support Vector Machine, CA = Classification Accuracy, and AUC = Area Under the Curve.						

In Table 2, an average accuracy of more than 95% was obtained in all the parameters evaluated. The parameters included AUC, CA, F1, Specificity, Precision and Recall. Specificity has the highest average accuracy of 99.8% followed by AUC with of 99.1%. CA and F1 had the least accuracy (in Table 2) as 95.0%. A closer look at each model indicated that KNN has the least accuracies in CA, F1, Precision and Recall. Although the pooled average in KMCM was the same as PCA's, they cannot be directly compared because different models were used in their analysis. KMCM, however, presented a very useful and explanatory analysis of the datasets compared with HCA.

Another KMCM-based analysis was performed to evaluate the models and parameters for T1, T2 and fused (F1) datasets. Data from T1 and T2 were analysed separately for the four models: KNN, SGD, NN and SVM. The evaluation results are presented in Tables 3 and 4 for T1 and T2, respectively.

Table 3. Evaluation results for Lateral Sensor (T1) data using K-Means Clustering Method (KMCM).

Models	**AUC (%)**	**CA (%)**	**F1 (%)**	**Precision (%)**	**Recall (%)**	**LogLoss (%)**	**Specificity (%)**
KNN	99.5	95.4	95.4	95.5	95.4	0.4	99.5
SVM	100.0	97.7	97.7	97.8	97.7	0.1	99.7
SGD	98.7	97.6	97.6	97.6	97.6	0.8	99.7
Neural Network	100.0	98.1	98.1	98.1	98.1	0.1	99.8
Average	**99.6**	**97.2**	**97.2**	**97.2**	**97.2**	**0.4**	**99.7**
Legend	KNN = K-Nearest Neighbors, NN = Neural Network, SGD – Stochastic Gradient Descent, SVM – Support Vector Machine, CA = Classification Accuracy, and AUC = Area Under the Curve.						

Table 4. Evaluation results for Ceiling Sensor (T2) data using K-Means Clustering Method (KMCM).

Models	**AUC (%)**	**CA (%)**	**F1 (%)**	**Precision (%)**	**Recall (%)**	**LogLoss (%)**	**Specificity (%)**
KNN	97.8	88.3	88.3	88.5	88.3	1.3	98.7
SVM	99.8	94.3	94.4	94.4	94.3	0.2	99.4
SGD	96.9	94.4	94.4	94.4	94.4	2.0	99.4
Neural Network	98.5	95.2	95.2	95.2	95.2	0.2	99.5
Average	**98.3**	**93.1**	**93.1**	**93.1**	**93.1**	**0.9**	**99.3**
Legend	KNN = K-Nearest Neighbors, NN = Neural Network, SGD – Stochastic Gradient Descent, SVM – Support Vector Machine, CA = Classification Accuracy, and AUC = Area Under the Curve.						

In Table 3, AUC and Specificity's average accuracy are obtained as 99.6% and 99.7%, respectively. Comparing these values to those in Table 4 (98.3% and 99.3%), AUC and Specificity had their highest accuracies in Table 3. Also, the metrics (in Table 3), namely, CA, F1, Precision and Recall obtained accuracies that were 4.1% higher than those in Table

4. A combination of the averages of all the metrics (excluding LogLoss) in Tables 2, 3, and 4 is presented in Table 5.

Table 5. Evaluation results for Lateral (T1), Ceiling (T2) and fused (F1) datasets using K-Means Clustering Method (KMCM).

Models	**Lateral %**	**Ceiling %**	**Fusion %**
KNN	96.8	91.7	94.3
SVM	98.4	96.1	96.6
SGD	98.1	95.7	97.8
Neural Network	98.7	96.5	97.3
Mean Accuracy	**98.0**	**95.0**	**96.5**
Legend	KNN = K-Nearest Neighbors, NN = Neural Network, SGD = Stochastic Gradient Descent, SVM = Support Vector Machine, CA = Classification Accuracy, and AUC = Area Under the Curve.		

In Table 5, a combination of the parameters, AUC, CA, Precision, F1, Recall and Specificity, indicated that T1 has the highest accuracy in all the models compared with those from T2 and F1 datasets. In addition, the Mean accuracy for all the models indicated 98.0%, 95.0% and 96.5% for T1, T2 and F1 datasets, respectively. This implied that T1 obtained the highest Mean accuracy, followed by F1 and then T2. An interval plot can further illustrate the Mean accuracy of T1, T2 and F1 datasets as presented in Figure 13. It should be noted that the intervals were calculated using the pooled Standard Deviation (SD).

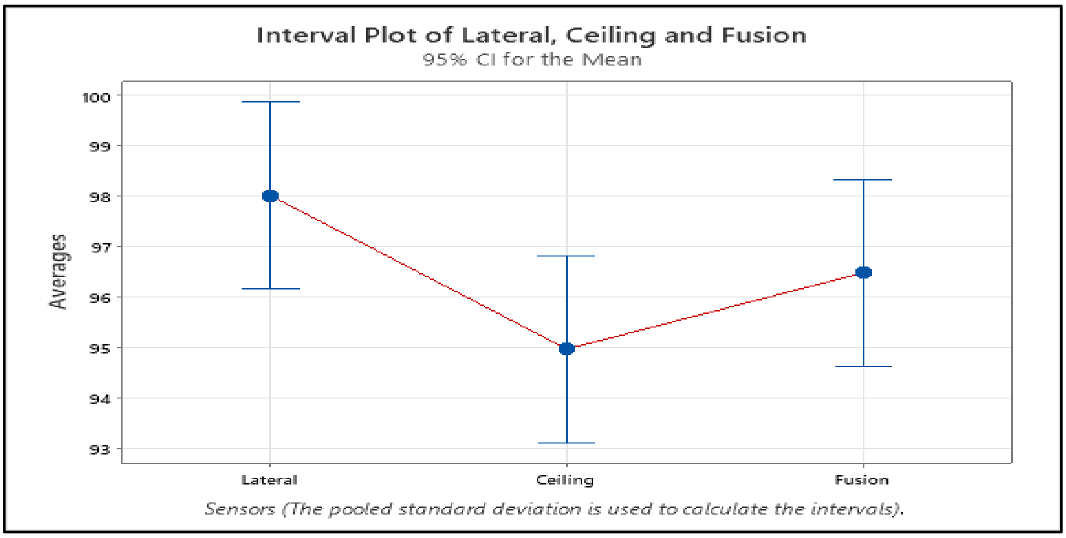

Figure 13. Interval plot of Lateral, Ceiling and Fused datasets computed from their pooled standard deviation.

Nevertheless, although previous analysis indicated a higher Mean average in favour of T1, one way ANOVA of the models in T1, T2, and F1 datasets using Welch's Test at 95% Confidence Interval indicated that there was no significant difference ($p = 0.105$) between the average values of the parameters. In addition, a 2-sample T-Test between T1 and F1, T2 and F1 indicated no significant difference between the fused data and those from individual SSs, $p = 0.08$ and 0.156, respectively. Further analysis with Grubbs' Test on T1, T2, and F1 datasets at a 5% significant level indicated no outlier in the Mean values of the datasets.

The pooled SD indicating the weighted average of the SDs for the three groups yielded a lower value of 1.5. In addition, the pooled Mean accuracy of all the models and parameters was obtained as 96.5%. Detailed analyses of the Mean values are presented in Table 6.

Table 6. Detailed analyses of Mean values from Lateral, Ceiling and Fused datasets using one way ANOVA.

Data Sources	Data points (N)	Mean Accuracy %	StDev	95% CI
Lateral	4	98.0	0.8	(96.1, 99.8)
Ceiling	4	95.0	2.2	(93.2, 96.9)
Fusion	4	96.5	1.5	(94.6, 98.4)
Averages	**4**	**96.5**	**1.5**	**(94.6, 98.4)**

5. Discussion and Conclusions

This study presented the fusion of data gleaned from USSs for the purposes of recognising and classifying indoor activities in home environments. It considered the use of DM models and methods for the cluster-based analysis of data obtained from the USSs. Results from data analysis demonstrated a pooled Mean accuracy of 96.5% for all the models and metrics considered in the study. Although the Mean accuracy in F1 data was slightly lower than in T1, a one-way ANOVA of the samples, T1, T2 and the F1 datasets indicated no significant difference between their Mean values. In addition, data fusion provided more information on instances of occlusion, which can make an incident go unnoticed.

The advantage of the proposed method in this work over other indoor activity recognition research [29], [37] include privacy-friendly postures and better accuracy. The accuracies obtained in this work can be compared with those obtained in [38], which used channel state information of a WiFi system to recognise activities such as lying down, standing, and walking. While the WiFi-based system has no information on the postural orientation of participants or the presence of hazardous objects, our model included privacy-friendly postures. Knowledge of the pose of room occupants and the surrounding objects can give further details, such as hot liquid spills, which can be hazardous to vulnerable individuals. The application of this study to smart homes and healthcare facilities can help encourage independent living [39]–[41].

One of the limitations of this study is the use of the contact sensors to determine if an occupant drank tea or coffee during the experiments since both (tea and coffee) were placed in the same cupboard. This implies that depending on the data from the thermal sensors alone, it would be difficult to determine if an occupant had tea or coffee. In a real-life setting, however, this confusion could be resolved if tea and coffee are placed on separate cupboards that are more than 1m apart. Another challenge with using the thermal sensors only without the contact sensors is on determining if the occupant used milk or cold water if both are placed in a similar container. To address this limitation in a real-life application, milk and cold water should be placed in containers of different sizes so that their blobs could be easily differentiated.

In conclusion, this study presented the use of low-cost unobtrusive (privacy-friendly) SSs for indoor ARC in a laboratory kitchen environment similar to a home environment. Experimental results indicated instances of activity recognition during activities such as making a cup of tea/coffee and classification of the same actions using DM models and methods with a pooled Mean predictive accuracy of 96.5%. Future study will calculate the speed and range of these activities, including the use of DM tools to score and evaluate their performance.

6. Acknowledgements

Research is funded by the EU's INTERREG VA program, managed by the Special EU Program Body (SEUPB).

References

[1] H. Medjahed, D. Istrate, J. Boudy, and B. Dorizzi, "Human activities of daily living recognition using fuzzy logic for elderly home monitoring," in *IEEE International Conference on Fuzzy Systems*, 2009, pp. 2001–2006, doi: 10.1109/FUZZY.2009.5277257.

[2] I. F. Ekerete, M. Garcia-Constantino, Y. Diaz, O. M. Giggins, M. A. Mustafa, A. Konios, P. Pouliet, C. D. Nugent, and J. McLaughlin, "Data Mining and Fusion of Unobtrusive Sensing Solutions for Indoor Activity Recognition," *Proc. Annu. Int. Conf. IEEE Eng. Med. Biol. Soc. EMBS*, vol. 2020-July, no. September, pp. 5357–5361, 2020, doi: 10.1109/EMBC44109.2020.9175896.

[3] M. K. Karlsson, T. Vonschewelov, C. Karlsson, M. CÃster, and B. E. Rosengen, "Prevention of falls in the elderly: A review," *Scand. J. Public Health*, vol. 41, no. 5, pp. 442–454, 2013, doi: 10.1177/1403494813483215.

[4] S. Myers, W. R. Grant, E. N. Lugn, B. Holbert, and C. J. Kvedar, "Impact of home-based monitoring on the care of patients with congestive heart failure," *Home Heal. Care Manag. Pract.*, vol. 18, no. 6, pp. 444–451, 2006, doi: 10.1177/1084822306289991.

[5] C. Debes, A. Merentitis, S. Sukhanov, M. Niessen, N. Frangiadakis, and A. Bauer, "Monitoring activities of daily living in smart homes: Understanding human behavior," *IEEE Signal Process. Mag.*, vol. 33, no. 2, pp. 81–94, Mar. 2016, doi: 10.1109/MSP.2015.2503881.

[6] M. Noorkõiv, H. Rodgers, and C. I. Price, "Accelerometer measurement of upper extremity movement after stroke: A systematic review of clinical studies," *J. Neuroeng. Rehabil.*, vol. 11, no. 1, 2014, doi: 10.1186/1743-0003-11-144.

[7] V. Lugade, E. Fortune, M. Morrow, and K. Kaufman, "Validity of using tri-axial accelerometers to measure human movement-Part I: Posture and movement detection," *Med. Eng. Phys.*, vol. 36, no. 2, pp. 169–176, 2014, doi: 10.1016/j.medengphy.2013.06.005.

[8] D. Figo, P. C. Diniz, D. R. Ferreira, and J. M. P. Cardoso, "Preprocessing techniques for context recognition from accelerometer data," *Pers. Ubiquitous Comput.*, vol. 14, no. 7, pp. 645–662, 2010, doi: 10.1007/s00779-010-0293-9.

[9] J. Oh, M. Eltoukhy, C. Kuenze, M. S. Andersen, and J. F. Signorile, "Comparison of predicted kinetic variables between Parkinson's disease patients and healthy age-matched control using a depth sensor-driven full-body musculoskeletal model," *Gait Posture*, vol. 76, pp. 151–156, Feb. 2020, doi: 10.1016/j.gaitpost.2019.11.011.

[10] Y. Kim, S. Baek, and B.-C. Bae, "Motion capture of the human body using multiple depth sensors," *ETRI J.*, vol. 39, no. 2, pp. 181–190, 2017, doi: 10.4218/etrij.17.2816.0045.

[11] J. Gangrade and J. Bharti, "Real time sign language recognition using depth sensor," *Int. J. Comput. Vis. Robot.*, vol. 9, no. 4, pp. 329–339, 2019, doi: 10.1504/IJCVR.2019.101527.

[12] B. Harasymowicz-Boggio, Ł. Chechliński, and B. Siemiątkowska, "Significance of features in object recognition using depth

sensors," *Opt. Appl.*, vol. 45, no. 4, pp. 559–571, 2015, doi: 10.5277/oa150411.

[13] R. I. Hg, P. Jasek, C. Rofidal, K. Nasrollahi, T. B. Moeslund, and G. Tranchet, "An RGB-D Database Using Microsoft's Kinect for Windows for Face Detection," in *2012 Eighth International Conference on Signal Image Technology and Internet Based Systems*, Nov. 2012, pp. 42–46, doi: 10.1109/SITIS.2012.17.

[14] R. Martin Martin, M. Lorbach, and O. Brock, "Deterioration of depth measurements due to interference of multiple RGB-D sensors," *IEEE Int. Conf. Intell. Robot. Syst.*, pp. 4205–4212, 2014, doi: 10.1109/IROS.2014.6943155.

[15] F. Riquelme, C. Espinoza, T. Rodenas, J. G. Minonzio, and C. Taramasco, "Ehomeseniors dataset: An infrared thermal sensor dataset for automatic fall detection research," *Sensors (Switzerland)*, vol. 19, no. 20, Oct. 2019, doi: 10.3390/s19204565.

[16] A. Kadambi, A. Bhandari, and R. Raskar, "3D Depth Cameras in Vision: Benefits and Limitations of the Hardware," pp. 3–26, 2014, doi: 10.1007/978-3-319-08651-4_1.

[17] M. Garcia-Constantino, A. Konios, I. Ekerete, S.-R. G. R. G. Christopoulos, C. Shewell, C. Nugent, and G. Morrison, "Probabilistic Analysis of Abnormal Behaviour Detection in Activities of Daily Living," *2019 IEEE Int. Conf. Pervasive Comput. Commun. Work. PerCom Work. 2019*, no. February, pp. 461–466, 2019, doi: 10.1109/PERCOMW.2019.8730682.

[18] M. Garcia-Constantino, A. Konios, M. A. Mustafa, C. Nugent, and G. Morrison, "Ambient and Wearable Sensor Fusion for Abnormal Behaviour Detection in Activities of Daily Living," *2020 IEEE Int. Conf. Pervasive Comput. Commun. Work. PerCom Work. 2020*, no. March, 2020, doi: 10.1109/PerComWorkshops48775.2020.9156249.

[19] M. Garcia-Constantino, A. Konios, and C. Nugent, "Modelling Activities of Daily Living with Petri nets," *2018 IEEE Int. Conf. Pervasive Comput. Commun. Work.*, no. i, pp. 866–871, 2018, doi: 10.1109/PERCOMW.2018.8480225.

[20] J. Wang, R. Chen, X. Sun, M. F. H. She, and Y. Wu, "Recognizing human daily activities from accelerometer signal," *Procedia Eng.*, vol. 15, pp. 1780–1786, 2011, doi: 10.1016/j.proeng.2011.08.331.

[21] Q. Ni, T. Patterson, I. Cleland, and C. Nugent, "Dynamic detection of window starting positions and its implementation within an activity recognition framework," *J. Biomed. Inform.*, vol. 62, pp. 171–180, 2016, doi: 10.1016/j.jbi.2016.07.005.

[22] L. Gao, A. K. Bourke, and J. Nelson, "Evaluation of accelerometer based multi-sensor versus single-sensor activity recognition systems," *Med. Eng. Phys.*, 2014, doi: 10.1016/j.medengphy.2014.02.012.

[23] B. Fida, I. Bernabucci, D. Bibbo, S. Conforto, and M. Schmid, "Varying behavior of different window sizes on the classification of static and dynamic physical activities from a single accelerometer," *Med. Eng. Phys.*, vol. 37, no. 7, pp. 705–711, 2015, doi: 10.1016/j.medengphy.2015.04.005.

[24] C. V. C. Bouten, K. T. M. Koekkoek, M. Verduin, R. Kodde, and J. D. Janssen, "A triaxial accelerometer and portable data processing unit for the assessment of daily physical activity," *IEEE Trans. Biomed. Eng.*, vol. 44, no. 3, pp. 136–147, 1997, doi: 10.1109/10.554760.

[25] J. W. Lockhart, T. Pulickal, and G. M. Weiss, "Applications of mobile activity recognition," *UbiComp'12 - Proc. 2012 ACM Conf. Ubiquitous Comput.*, pp. 1054–1058, 2012, doi: 10.1145/2370216.2370441.

[26] A. Konios, M. Garcia-Constantino, S.-R. G. Christopoulos, M. A. Mustafa, I. Ekerete, C. Shewell, C. Nugent, and G. Morrison, "Probabilistic Analysis of Temporal and Sequential Aspects of Activities of Daily Living for Abnormal Behaviour Detection," *Proc. 16th IEEE Int. Conf. Ubiquitous Intell. Comput. (UIC '19)*, pp. 723–730, 2019, doi: 10.1109/SmartWorld-UIC-ATC-SCALCOM-IOP-SCI.2019.00158.

[27] T. Shany, S. J. Redmond, M. Marschollek, and N. H. Lovell, "Assessing fall risk using wearable sensors: a practical discussion," *Z. Gerontol. Geriatr.*, vol. 45, no. 8, pp. 694–706, 2012, doi: 10.1007/s00391-012-0407-2.

[28] A. König, C. F. Crispim Junior, A. Derreumaux, G. Bensadoun, P. D. Petit, F. Bremond, R. David, F. Verhey, P. Aalten, and P. Robert, "Validation of an automatic video monitoring system for the detection of instrumental activities of daily living in dementia patients," *J. Alzheimer's Dis.*, vol. 44, no. 2, pp. 675–685, 2015, doi: 10.3233/JAD-141767.

[29] I. González-Díaz, V. Buso, J. Benois-Pineau, G. Bourmaud, G. Usseglio, R. Mégret, Y. Gaestel, and J. F. Dartigues,

"Recognition of instrumental activities of daily living in egocentric video for activity monitoring of patients with dementia," in *Health Monitoring and Personalized Feedback using Multimedia Data*, Springer International Publishing, 2015, pp. 161–178.

[30] C. D. Nugent, M. D. Mulvenna, X. Hong, and S. Devlin, "Experiences in the development of a Smart Lab," *Int. J. Biomed. Eng. Technol.*, vol. 2, no. 4, pp. 319–331, 2009, doi: 10.1504/IJBET.2009.027796.

[31] I. Cleland, S. McClean, J. Rafferty, J. Synnott, C. Nugent, A. Ennis, P. Catherwood, and I. McChesney, "A Scalable, Research Oriented, Generic, Sensor Data Platform," *IEEE Access*, vol. 6, pp. 45473–45484, 2018, doi: 10.1109/ACCESS.2018.2852656.

[32] J. Rafferty, J. Medina-Quero, S. Quinn, C. Saunders, I. Ekerete, C. Nugent, J. Synnott, and M. Garcia-Constantino, "Thermal Vision Based Fall Detection via Logical and Data driven Processes," *Proc. - 2019 IEEE/ACIS 4th Int. Conf. Big Data, Cloud Comput. Data Sci. BCD 2019*, pp. 35–40, 2019, doi: 10.1109/BCD.2019.8884820.

[33] P. Bhatia, "Introduction to Data Mining," *Data Min. Data Warehous.*, no. May, pp. 17–27, 2019, doi: 10.1017/9781108635592.003.

[34] L. Morissette and S. Chartier, "The k-means clustering technique: General considerations and implementation in Mathematica," *Tutor. Quant. Methods Psychol.*, vol. 9, no. 1, pp. 15–24, 2013, doi: 10.20982/tqmp.09.1.p015.

[35] S. Hosseini and S. R. Sardo, "Data mining tools -a case study for network intrusion detection," *Multimed. Tools Appl.*, vol. 80, no. 4, pp. 4999–5019, 2021, doi: 10.1007/s11042-020-09916-0.

[36] M. Rayed Bin Wahed, "Comparative Analysis between Inception-V3 and Other Learning Systems using Facial Expressions Detection," pp. 1–48, 2016.

[37] B. Delachaux, J. Rebetez, A. Perez-Uribe, and H. F. Satizábal Mejia, "Indoor activity recognition by combining One-vs.-All neural network classifiers exploiting wearable and depth sensors," *Lect. Notes Comput. Sci. (including Subser. Lect. Notes Artif. Intell. Lect. Notes Bioinformatics)*, vol. 7903 LNCS, no. PART 2, pp. 216–223, 2013, doi: 10.1007/978-3-642-38682-4_25.

[38] M. A. A. Al-qaness, F. Li, X. Ma, Y. Zhang, and G. Liu, "Device-free indoor activity recognition system," *Appl. Sci.*, vol. 6, no. 11, pp. 1–13, 2016, doi: 10.3390/app6110329.

[39] A. Arcelus, R. Goubran, M. H. Jones, and F. Knoefel, "Integration of smart home technologies in a health monitoring system for the elderly," *Proc. - 21st Int. Conf. Adv. Inf. Netw. Appl. Work. AINAW'07*, vol. 1, pp. 820–825, 2007, doi: 10.1109/AINAW.2007.209.

[40] A. Lotfi, C. Langensiepen, S. M. Mahmoud, and M. J. Akhlaghinia, "Smart homes for the elderly dementia sufferers: Identification and prediction of abnormal behaviour," *J. Ambient Intell. Humaniz. Comput.*, vol. 3, no. 3, pp. 205–218, 2012, doi: 10.1007/s12652-010-0043-x.

[41] J. Ancheta, M. Husband, D. Law, and M. Reding, "Initial functional independence measure score and interval post stroke help assess outcome, length of hospitalization, and quality of care.," *Neurorehabil. Neural Repair*, vol. 14, no. 2, pp. 127–134, 2000, doi: 10.1177/154596830001400205.

[42] Y. Wang, J. Li, G. Liu, and P. Stoica, "Polarimetric SAR target feature extraction and image formation via semi-parametric methods," *Digit. Signal Process. A Rev. J.*, vol. 14, no. 3, pp. 268–293, 2004, doi: 10.1016/j.dsp.2003.09.001.